

LEVEL 11

12

THE VIEWS AND CONCLUSIONS CONTAINED IN THIS DOCUMENT ARE THOSE OF THE AUTHOR AND SHOULD NOT BE INTERPRETED AS NECESSARILY REPRESENTING THE OFFICIAL POLICIES, EITHER EXPRESSED OR IMPLIED, OF THE ADVANCED RESEARCH PROJECTS AGENCY OR THE U.S. GOVERNMENT.

SC A047212

ADA 085456

EXCIMER LASER RESEARCH

J. H. Parks and D. Klimek
AVCO EVERETT RESEARCH LABORATORY, INC.
2385 Revere Beach Parkway
Everett, MA 02149

Mid-Term Report for Period 16 November 1977 to 15 May 1978

DTIC
ELECTE
JUN 12 1980
C

APPROVED FOR PUBLIC RELEASE; DISTRIBUTION UNLIMITED.

Sponsored by
DEFENSE ADVANCED RESEARCH PROJECTS AGENCY
ARPA Order No. 1806

Monitored by
OFFICE OF NAVAL RESEARCH
DEPARTMENT OF THE NAVY
Arlington, VA 22217

80 6 12 006

DC FILE COPY

FOREWORD

DARPA Order No.: 1806

Program Code No.: 5E20

Name of Contractor: Avco Everett Research Laboratory, Inc.

Effective Date of Contract: 15 August 1974

Contract Expiration Date: 29 September 1979

Amount of Contract: \$1,146,990

Contract No.: N00014-75-C-0063

Principal Investigator and Phone No.: J. H. Parks
(617) 389-3000 Ext. 323

Scientific Officer: Director, Physics Program
Physical Sciences Division
Office of Naval Research
Department of the Navy
800 North Quincy Street
Arlington, VA 22217

Short Title of Work: Excimer Laser Research

UNCLASSIFIED

SECURITY CLASSIFICATION OF THIS PAGE (When Data Entered)

REPORT DOCUMENTATION PAGE		READ INSTRUCTIONS BEFORE COMPLETING FORM	
1. REPORT NUMBER	2. GOVT ACCESSION NO.	3. RECIPIENT'S CATALOG NUMBER	
	AD-A085456		
4. TITLE (and Subtitle)		5. TYPE OF REPORT & PERIOD COVERED	
(6) EXCIMER LASER RESEARCH		(9) Mid-Term Report 16 Nov 1977-15 May 1978	
7. AUTHOR(s)		8. CONTRACT OR GRANT NUMBER(s)	
(10) J.H. Parks and D./Klimek		(15) N00014-75-C-0063, DARPA Order-1806	
9. PERFORMING ORGANIZATION NAME AND ADDRESS		10. PROGRAM ELEMENT, PROJECT, TASK AREA & WORK UNIT NUMBERS	
Avco Everett Research Laboratory, Inc. 2385 Revere Beach Parkway Everett, MA 02149		(12) 37	
11. CONTROLLING OFFICE NAME AND ADDRESS		12. REPORT DATE	
Defense Advanced Research Projects Agency DARPA Order No. 1806		(11) 15 May 78	
14. MONITORING AGENCY NAME & ADDRESS (if different from Controlling Office)		13. NUMBER OF PAGES	
Office of Naval Research Department of the Navy Arlington, VA 22217		32	
		15. SECURITY CLASS. (of this report)	
		Unclassified	
		15a. DECLASSIFICATION/DOWNGRADING SCHEDULE	
16. DISTRIBUTION STATEMENT (of this Report)			
Approved for public release; distribution unlimited.			
17. DISTRIBUTION STATEMENT (of the abstract entered in Block 20, if different from Report)			
18. SUPPLEMENTARY NOTES			
19. KEY WORDS (Continue on reverse side if necessary and identify by block number)			
Excimer Lasers Electron Beams Mercury Halides Mercury Halide Radiative Lifetimes Mercury Halide Formation Kinetics Mercury Halide Quenching			
20. ABSTRACT (Continue on reverse side if necessary and identify by block number)			
This mid-term report describes theoretical and experimental investigations of the mercury monohalides. These molecules show great promise for achieving high power scalable laser action in the visible portion of the spectrum. The report includes an analysis of formation kinetics; theoretical calculations of the mercury halide radiative lifetimes; and an			

DD FORM 1 JAN 73 1473

EDITION OF 1 NOV 65 IS OBSOLETE

UNCLASSIFIED

SECURITY CLASSIFICATION OF THIS PAGE (When Data Entered)

048450

JCB

UNCLASSIFIED

SECURITY CLASSIFICATION OF THIS PAGE(When Data Entered)

↓(20)

experimental determination of the heavy particle quenching of
HgX^γ(B) by mercury atoms.



UNCLASSIFIED

SECURITY CLASSIFICATION OF THIS PAGE(When Data Entered)

TABLE OF CONTENTS

<u>Section</u>	<u>Page</u>
List of Illustrations	3
I. MERCURY HALIDE RESEARCH	5
A. HgX* Formation Kinetics	5
1. Ion-Ion Recombination	5
2. Exchange Reactions and Interception	5
3. Neutral Channels	8
4. HgX* Intrinsic Efficiency	10
B. Mercury Halide Radiative Lifetimes	12
C. HgX* Quenching by Hg	20
REFERENCES	31

Accession For	
NTIS GRA&I	<input checked="" type="checkbox"/>
DDC TAB	<input type="checkbox"/>
Unannounced	<input type="checkbox"/>
Justification	
By _____	
Distribution/	
Availability Codes	
Dist	Avail and/or special
A	

LIST OF ILLUSTRATIONS

<u>Figure</u>		<u>Page</u>
1	Ion-Ion Recombination Channel Suggested for HgCl* Formation in Ar/Xe/Hg/CCl ₄ Mixtures	7
2	HgCl* Formation vis Exchange Reactions in Ar/Xe/Hg/CCl ₄ Mixtures	9
3	Suggested Formation Channels for Dominant Species which Absorb at the Laser Wavelength λ_L In Ar/Xe/Hg/CCl ₄ Mixtures	11
4	B \rightarrow X Radiative Lifetime of HgX* as a Function of the Ionic Mixing Coefficient, β	18
5	Schematic of the Experimental Apparatus	21
6	Oscillogram of a Typical HgCl* Signal and the Associated Trace of E-Beam Current Density	22
7	Plot of Experimental Data Showing Best Linear Fit and the Resulting Quenching Rate Constant k_1	25
8	Plot of Experimental Data Showing Best Linear Fit and the Resulting Quenching Rate Constant k_2	26
9	HgCl* Fluorescence vs Helium Pressure at Mercury Densities Corresponding to 45.5 and 22.3 Torr	28

I. MERCURY HALIDE RESEARCH

A. HgX* FORMATION KINETICS

A detailed study of the HgCl and HgBr molecular kinetics with e-beam excitation has not yet been performed. However, we will summarize the relative importance of several formation channels of HgCl* which are consistent with lasing and fluorescence data. These formation kinetics are summarized in Table 1.

1. Ion-Ion Recombination

The dominant formation channel of HgCl* under our excitation conditions is the rapid three-body recombination of Hg⁺ ions with Cl⁻ ions. The suggested ion-ion kinetic channeling is outlined in Figure 1. In gas mixtures containing high-pressure xenon, the high-energy beam electrons deposit most of their energy into the formation of Xe⁺. The xenon ions and neutrals form Xe₂⁺ with a three-body rate constant of $3.6 \times 10^{-31} \text{ cm}^6/\text{s}$.⁽¹⁾ The Xe₂⁺ can then undergo charge transfer with Hg to form Hg⁺ which is energetically near resonance, $\Delta E = 0.8 \text{ eV}$ (exothermic). This reaction may exhibit a comparable rate⁽²⁾ to an analogous, near resonant charge transfer reaction involving Ar₂⁺ and Kr which forms Kr⁺ with a rate constant of $7.5 \times 10^{-10} \text{ cm}^3/\text{s}$.⁽³⁾ The Cl⁻ ions is formed by rapid dissociative attachment⁽⁴⁾ of secondary electrons to CCl₄. The HgCl* ionic state is then formed by ion-ion recombination of Hg⁺ and Cl⁻ which can have an effective two body rate constant of $10^{-6} \text{ cm}^3/\text{s}$ at pressure of interest.⁽⁵⁾ In the Ar/Xe gas mixtures, the observed increase in HgCl* fluorescence is consistent with an enhanced formation of Hg⁺. This could occur via additional charge transfer reactions involving Ar₂⁺ and Xe which increase Xe₂⁺ density and the Hg⁺ as discussed above.

2. Exchange Reactions and Interception

Fluorescence spectra obtained from Ar/Hg/CCl₄ and Xe/Hg/CCl₄ mixtures clearly indicate the formation of ArCl* and XeCl*.

TABLE 1. HgCl* FORMATION KINETICS ACTIVE IN Ar/Xe/Hg/CCl₄ E-BEAM PUMPED MIXTURES

ION-ION RECOMBINATION

$e + Ar$	$\rightarrow Ar^+ + e + e_s$	$10^{23} cm^{-3} sec^{-1}$
$Ar^+ + 2Ar$	$\rightarrow Ar_2^+ + Ar$	$2.5 \times 10^{-31} cm^6 sec^{-1}$
$Xe^+ + 2Xe$	$\rightarrow Xe_2^+ + Xe$	$3.6 \times 10^{-31} cm^6 sec^{-1}$
$Ar_2^+ + Xe$	$\rightarrow ArXe^+ + Ar$	} $\sim 2 \times 10^{-10} cm^3 sec^{-1}$
$ArXe^+ + Xe$	$\rightarrow Xe_2^+ + Ar$	
$Xe_2^+ + Hg$	$\rightarrow Hg^+ + 2Xe$	$\sim 3 \times 10^{-10} cm^3 sec^{-1}$

$e_s + Ar_2^+$	$\rightarrow Ar^{**} + Ar$	$6 \times 10^{-7} cm^3 sec^{-1}$
$e_s + Xe_2^+$	$\rightarrow Xe^{**} + Xe$	$2 \times 10^{-7} cm^3 sec^{-1}$
$Ar^* + 2Ar$	$\rightarrow Ar_2^* + Ar$	$10^{-32} cm^6 sec^{-1}$
$Xe^* + 2Xe$	$\rightarrow Xe_2^* + Xe$	$5 \times 10^{-32} cm^6 sec^{-1}$

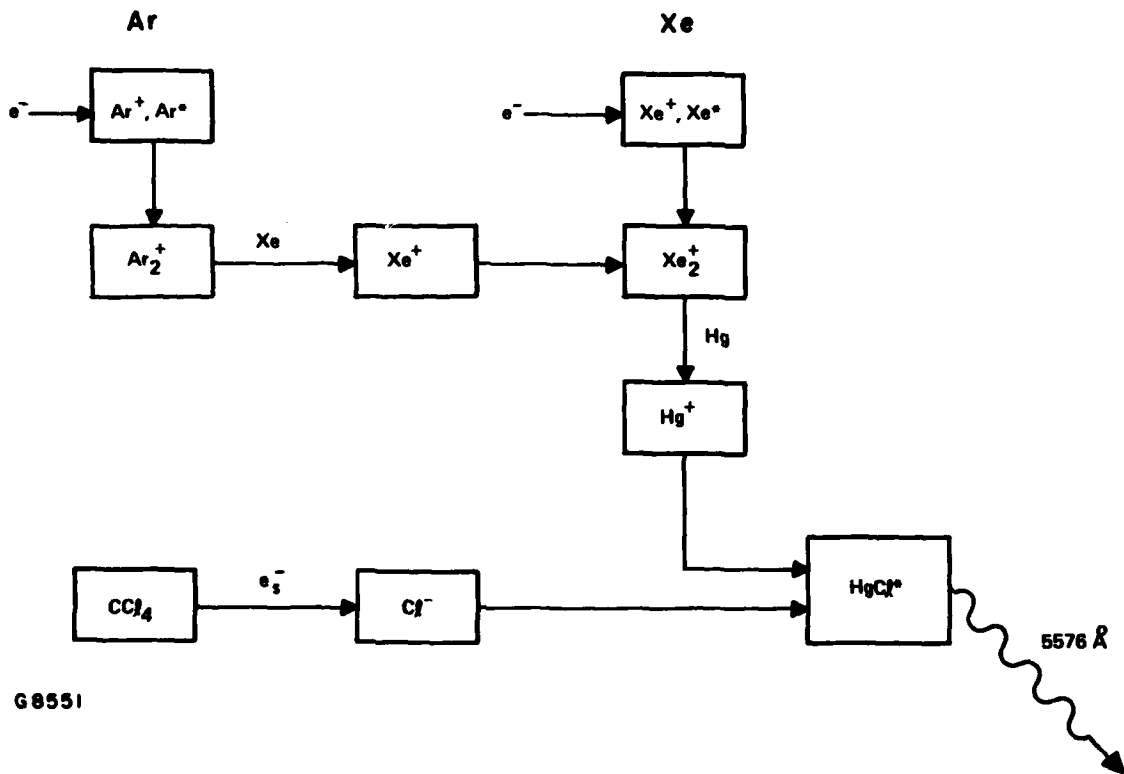
$e_s + CCl_4$	$\rightarrow Cl^- + CCl_3$	$10^{-7} cm^3 sec^{-1}$
$Hg^+ + Cl^- + Ar$	$\rightarrow HgCl^* + Ar$	$\sim 10^{-6} cm^3 sec^{-1}$
$HgCl^*$	$\rightarrow h\nu (5576 \text{ \AA}) + HgCl$	22 nsec

EXCHANGE REACTION

$Ar^+ + Cl^- + Ar$	$\rightarrow ArCl^* + Ar$	} $\sim 10^{-6} cm^3 sec^{-1}$
$Ar_2^+ + Cl^-$	$\rightarrow ArCl^* + Ar$	
$ArCl^*$	$\rightarrow h\nu (1750 \text{ \AA}) + Ar + Cl$	10 nsec
$Xe^+ + Cl^- + Ar$	$\rightarrow XeCl^* + Ar$	} $\sim 10^{-6} cm^3 sec^{-1}$
$Xe_2^+ + Cl^-$	$\rightarrow XeCl^* + Xe$	
$XeCl^*$	$\rightarrow h\nu (3080 \text{ \AA}) + Xe + Cl$	16 nsec
$Hg + ArCl^*$	$\rightarrow HgCl^* + Ar$	
$Hg + XeCl^*$	$\rightarrow HgCl^* + Xe$	

NEUTRAL REACTION

$Hg^* + CCl_4$	$\rightarrow HgCl^* + CCl_3$	$\sigma = 34 (\text{ \AA})^2$
----------------	------------------------------	-------------------------------



G8551

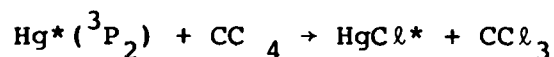
Figure 1. Ion-Ion Recombination Channel Suggested for HgCl* Formation in Ar/Xe/Hg/CCl₄ Mixtures

Displacement reactions can follow in which mercury exchanges with these excited molecules to form HgCl^* as shown in Figure 2. The rate constant for an analogous reaction involving Kr and ArF^* has been measured⁽⁶⁾ to be $6.5 \times 10^{-10} \text{ cm}^3/\text{sec}$. It is expected that XeCl^* would be a more efficient precursor since dissociation to $\text{Xe} + \text{Cl}^*$ should have a smaller rate constant than the dissociation of ArCl^* to $\text{Ar} + \text{Cl}^*$. Although the relative importance of this HgCl^* formation channel has not been determined, the competing radiative processes of ArCl^* and XeCl^* suggest that displacement reactions will not be dominant. A preliminary measurement of XeCl^* quenching by Hg, performed in this program, indicates that the branching into HgCl^* via $\text{XeCl}^* + \text{Hg} \rightarrow \text{HgCl}^* + \text{Xe}$ is between 10-50%.

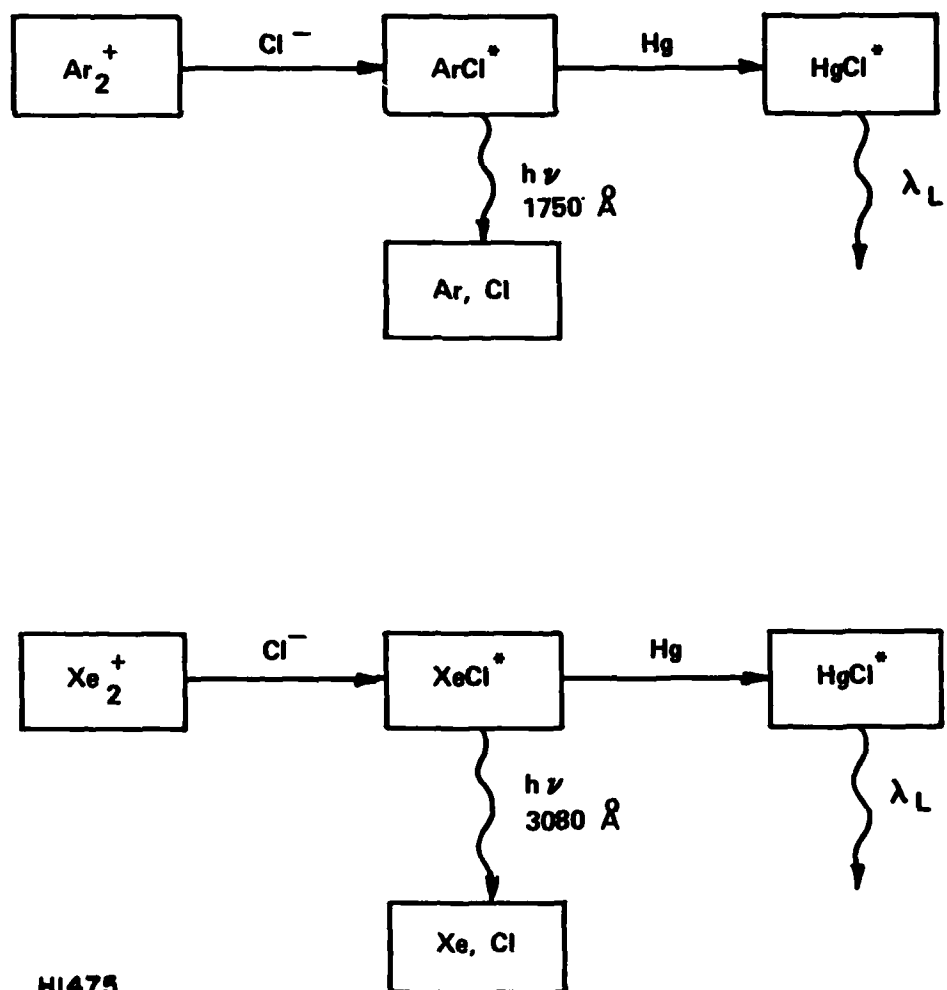
The formation of a triatomic species, Kr_2F^* in KrF laser mixtures has been observed.⁽⁷⁾ In this case, the triatomic formation is saturable since Kr_2F^* formation depends on the density of KrF^* which is driven down by the intense laser flux. Similar processes could be present in mercury halide laser mixtures. If Hg_2Cl^* is formed, it will probably fluoresce in the near infrared $\geq 7000 \text{ \AA}$.

3. Neutral Channels

The mercury metastable channel leading to HgCl^* through reaction



has been observed⁽⁸⁾ to have a reactive cross section of 34 (\AA)^2 and a branching ratio into the upper laser level of near unity. Since the energies of the mercury metastables $\text{Hg}^*(^6\text{P})$ are about 5 eV, this reaction suggests the possibility of efficient discharge pumping of HgCl^* . However, this is probably not an important formation process for e-beam pumping. The fluorescence data from laser mixtures indicates only weak emission from higher lying mercury levels such as 7^3S_1 which populate the 6^3P



HI475

Figure 2. HgCl^* Formation via Exchange Reactions in Ar/Xe/Hg/CCl_4 Mixtures

metastables. When the CCl_4 density is decreased by an order of magnitude, to about 1 Torr, the emission from HgCl^* shows a comparable reduction but mercury emission from 7^3S_1 increases significantly. Thus, for laser gas mixtures the neutral channel kinetics do not appear to lead to efficient mercury metastable production under these excitation conditions. It is interesting to note that the use of HBr in HgBr lasing mixtures eliminates the Hg^* metastable channel because the 3.8 eV H-Br bond strength renders the above neutral reaction endothermic by roughly .5 eV.

The absence of lasing in pure Ar mixtures and the observed weak lasing in pure Xe mixtures suggests the possibility that absorption by Ar_2^* and Xe_2^* may be competing with the HgCl^* and HgBr^* stimulated emission as outlined in Figure 3. The fluorescence from pure Ar and pure Xe mixtures were comparable for similar e-beam energy deposition. Strong visible absorption identified with these rare gas excimers has been observed⁽⁹⁾ during e-beam excitation in high pressure Ar and also in Xe. However, in Ar/Xe/Hg/ CCl_4 gas mixtures the strong Ar_2^* absorption is possibly reduced via the rapid quenching^(10,11) of Ar_2^* by Xe.

4. HgX* Intrinsic Efficiency

Lasing on the HgCl^* and HgBr^* band transitions introduces new high-power laser sources at visible wavelengths. The detailed molecular kinetics in these gas mixtures have yet to be established in order to assess the possible efficiency and scalability of these lasers. The measured intrinsic efficiencies are the result of increased output coupling. The optimization of laser mixtures and pumping power presently underway should result in higher values. In pure e-beam pumping, the maximum effective quantum efficiency of 9% is limited by the 26 eV needed to form an argon ion. Thus, the observed value of 3.8% indicates efficient HgCl^* formation. If a discharge were used to pump the Hg^* (6_p) metastable levels directly and form HgX^* via neutral reactions such as the effective quantum efficiency would be roughly 50%.

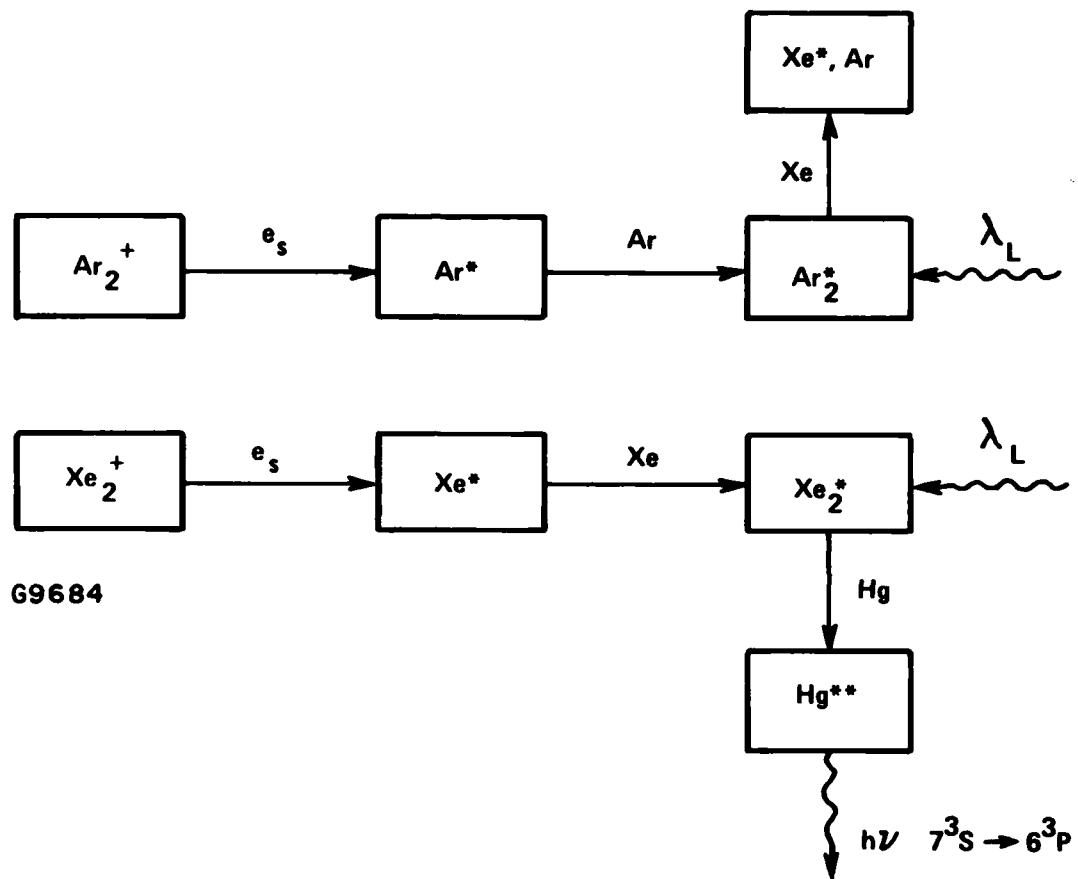


Figure 3. Suggested Formation Channels for Dominant Species which Absorb at the Laser Wavelength λ_L in Ar/Xe/Hg/ CCl_4 Mixtures

B. MERCURY HALIDE RADIATIVE LIFETIMES

This section will discuss the application of a charge transfer model to calculate the oscillator strengths and radiative lifetimes for the mercury-monohalide laser transitions $B^2\Sigma_{1/2}^+ - X^2\Sigma_{1/2}^+$. To our knowledge, no previous calculations of the radiative lifetimes of these systems have been attempted. Dunning and Hay⁽¹²⁾ have performed ab initio calculations for KrF, in which they computed both the potential energy curves and oscillator strengths. Their calculation involved an extensive configuration-interaction treatment, utilizing between 2000-3000 configurations. Although such calculations are valuable, they are enormously time consuming and must be applied individually to each state of each rare gas-halide pair. This approach is clearly not in a form from which general conclusions can be drawn and applied to the whole class of rare gas-halide systems. It would therefore be desirable to have available a simpler model, from which one can make fairly reliable predictions for a wide range of systems. The simple charge transfer theory developed originally by Mulliken⁽¹³⁾ and used by Zare and Herschbach⁽¹⁴⁾ for the alkali halides, appears to be a scheme capable of being generalized to a wide variety of systems for which the "ionic-bonding" model holds, including the alkali halides, rare gas-halides, and mercury-monohalides. The alkali-halide analogy has been extremely successful⁽¹⁵⁾ in predicting the properties of the rare gas-halides, and the use of the charge transfer model to calculate the transition strengths can be thought of as simply an extension of the analogy.

The basic idea behind the charge transfer theory is that the electron initially localized around the halogen center, in the upper M^+X^- state, "jumps" or is transferred to the mercury positive ion, filling the p-state vacancy, and thus ending up in the MX atomic ground state. This is essentially a "valence bond" picture, in which the electron is transferred from one atomic center to the other. For example, in the mercury chloride

B → X transition an electron which is initially localized on the Cl atom, forming Cl⁻, is transferred to the Hg⁺ ion resulting in the ground state configuration of mercury chloride.

In general, the mercury-halides are closely analogous in structure to the rare gas-halides. The upper laser level is "ionic", while the ground state is primarily "atomic". There are, however, some significant differences between the two systems. The upper level of the mercury-halides correlates with the Hg⁺(²S_{1/2}) + X⁻(¹S₀) atomic states so that only a single ²Σ_{1/2} ionic state is formed. The ground state correlates with the Hg(¹S₀) + X(²P_{3/2, 1/2}) atomic limit, so that we obtain ²Π_{1/2} and ²Σ_{1/2} molecular states, as in the case of the rare gas-halides. A more important difference is that the ground states of the mercury-halides are essentially bound states with the binding energy ranging from⁽¹⁶⁾ 0.36 eV for HgI to 1.04 eV for HgCl. With the exception of XeF, which is slightly bound, all of the rare gas-halide ground states are repulsive.

Although the upper and lower states are predominantly ionic and covalent, respectively, it proves to be essential to allow for mixing between these states in order to obtain reasonable results from the theory. The mixed X and B state wavefunctions can be expressed as

$$\begin{aligned}\psi_B &= N_B (\psi^i + \alpha \psi^c), \\ \psi_X &= N_X (\psi^c - \beta \psi^i),\end{aligned}\tag{1}$$

with $\alpha = (\beta - S)/(1 - \beta S)$, and where ψ^i and ψ^c are the purely ionic and covalent wavefunctions, N_B and N_X are normalization constants, S is the overlap integral between ψ^i and ψ^c , and β is the mixing coefficient. Except for very large values of the internuclear distance, S is non-zero so that S as well as β must appear in the expression for α in order to make the

initial and final wavefunctions orthogonal. A major difficulty in the theory is the specification of the mixing parameter β . Given the lack of data on the mercury-monohalides, we have used the procedure outlined by Coulson⁽¹⁷⁾ to estimate the degree of ionic character of the ground state from the electronegativities of the mercury and halogen atoms. The values for the percent ionic character [i.e., $100 \beta^2 / (1 + \beta^2)$] obtained in this way are given in Table 2. The electronegativities can also be used to determine the so-called covalent-ionic resonance energy, Δ , which is simply the ionic contribution to the binding energy. The values of Δ (in eV) turn out to be 1.2, 0.81, and 0.36 for HgCl, HgBr, and HgI, respectively, as compared to the experimental dissociation energies (in eV) of 1.0, 0.7, and 0.36. It may thus be inferred that the electronegativity method tends to overestimate the mixing parameter.

In order to complete the definition of the wavefunctions in Eq. (1) it remains to determine the one-electron orbitals that make up ψ^c and ψ^i . In keeping with the valence bond picture we have adopted, ψ^c and ψ^i are simply taken to be products of unperturbed atomic (ionic) wavefunctions. The analytic Hartree-Fock functions of Clementi and Roetti⁽²¹⁾ were used for the atomic and ionic halogen wavefunctions. Unfortunately, no such functions exist for neutral or singly-ionized mercury. A further complication arises from the fact that relativistic effects are non-negligible for the mercury valence orbital. Since the valence electrons are in an s-state, the most important relativistic effect⁽²²⁾ is a contraction of the radial wavefunction toward the nucleus, due to the absence of a repulsive angular momentum barrier. We have therefore calculated a non-relativistic Hartree-Fock-Slater (HFS) wavefunction, utilizing the Herman-Skillman computer program,⁽²³⁾ and scaled the function according to the formula

$$P'(r) = \gamma^{1/2} P_{\text{non-rel.}}(\gamma r)$$

TABLE 2. PARAMETERS FOR THE B-X TRANSITION IN THE Hg-HALIDES

	α	β	S	X^2_{Σ}	Percent Ionic Character	B^2_{Σ}	Internuclear Equilibrium Distance (Å)	λ (Å)	μ (Debye)	τ (nsec)		Ref.
										Theory	Expt.	
HgCl ₂	-.64	.53	.87	22	3.15	5576	-6.60	20	22.2	(18)		
HgBr ₂	-.59	.45	.82	17	3.24	5018	-6.32	16	23.7	(19,20)		
HgI ₂	-.51	.35	.73	11	3.50	4412	-5.92	12	27.3	(20)		

so as to reproduce the expectation values $\langle r^n \rangle$ tabulated by Lu et al, ⁽²⁴⁾ from their relativistic HFS program. The calculation was made for $n = -1, 1, 2$ and in all cases $\gamma \approx 1.16$ for Hg; the same value was used for Hg^+ . The final function, $P'(r)$, were then represented by a sum of Slater-type orbitals (STOs) using a nonlinear least squares fitting procedure. The basis set for the 6s functions of Hg and Hg^+ consisted of eight STOs.

With the wavefunctions given in Eq. (1), the transition dipole moment can be reduced to an expression involving only one-electron terms. Consider that the ionic and covalent molecular wavefunctions ψ^i and ψ^c are expressed in terms of products of atomic wavefunctions ϕ for Hg, Hg^+ , X and X^- ($X = \text{Cl}, \text{Br}, \text{I}$) by

$$\begin{aligned}\psi^i &= (\phi_{\text{Hg}^+}) \cdot (\phi_{X^-}) \\ \psi^c &= (\phi_{\text{Hg}}) \cdot (\phi_X).\end{aligned}\tag{2}$$

These atomic wavefunctions ϕ are represented by Hartree-Fock functions composed of products of one-electron wavefunction, ϕ . Then, the transition dipole moment μ can be shown to be given by

$$\begin{aligned}\mu &= N_B N_X [\langle \phi_{\text{Hg}} | r | \phi_{X^-} \rangle (1-\alpha\beta)\chi \\ &+ \alpha \langle \phi_{\text{Hg}} | r | \phi_{\text{Hg}} \rangle - \beta \langle \phi_{X^-} | r | \phi_{X^-} \rangle],\end{aligned}\tag{3}$$

where ϕ_{X^-} is the initial wavefunction of the active electron centered on the negative halogen ion (X^-), ϕ_{Hg} is the final state one-electron wavefunction, r is the position vector, and χ is an overlap integral involving all of the electron orbitals not involved in the transition. All two-center integrals were evaluated from an expansion developed by Sharma ⁽²⁵⁾ for the case of one-electron wavefunctions expressed as a sum of STOs.

The calculation of the overlap function $S \equiv \langle \psi^i | \psi^c \rangle$ and the parameter α for various mercury monohalides are given in Table 2. All these calculations depend on a choice of molecular internuclear separation. An experimental value for the equilibrium internuclear distance exists⁽²⁶⁾ for the ionic state of HgCl, but not for the other halides. In order to estimate these distances, the relative sizes of the alkali halides were used as a guide. It was found that the internuclear separation of the alkali bromides are $\approx 3\%$ larger than those of the alkali chlorides while the iodides are $\approx 12\%$ larger. The internuclear distances of the Hg-halides were scaled accordingly, and are given in Table 2.

The results of the calculations for the B \rightarrow X transitions are summarized in Table 2. The radiative lifetime of the transition is given, in terms of the quantity μ , by $\tau = 3h\lambda^3/64\pi^4\mu^2$ where λ is the transition wavelength. The model predicts a decrease in lifetime with increasing halogen size due to the λ^3 dependence. There is a competing trend caused by a decrease in the dipole matrix element, but this effect is much weaker. In Table 2, we also show results of experimental measurements of the HgX radiative lifetimes. Theory and experiment are in good agreement for HgCl. The theoretical value is only $\sim 30\%$ lower than the measured value for HgBr and $\sim 50\%$ lower for HgI which is quite satisfactory considering the simplicity of the model. Further calculations were carried out to test the sensitivity of the results to the various parameters. When the internuclear distance was varied by 5%, the lifetime changed by less than 5% in all cases. As discussed earlier, the mixing coefficients are the parameters which contain the greatest uncertainty. To give some idea of the sensitivity of our calculation to the percent ionic character of the ground state, the radiative lifetime of each mercury monohalide is plotted as a function of the mixing coefficient in Figure 4. The value of the mixing coefficient inferred from the electronegativity is indicated for each molecule in

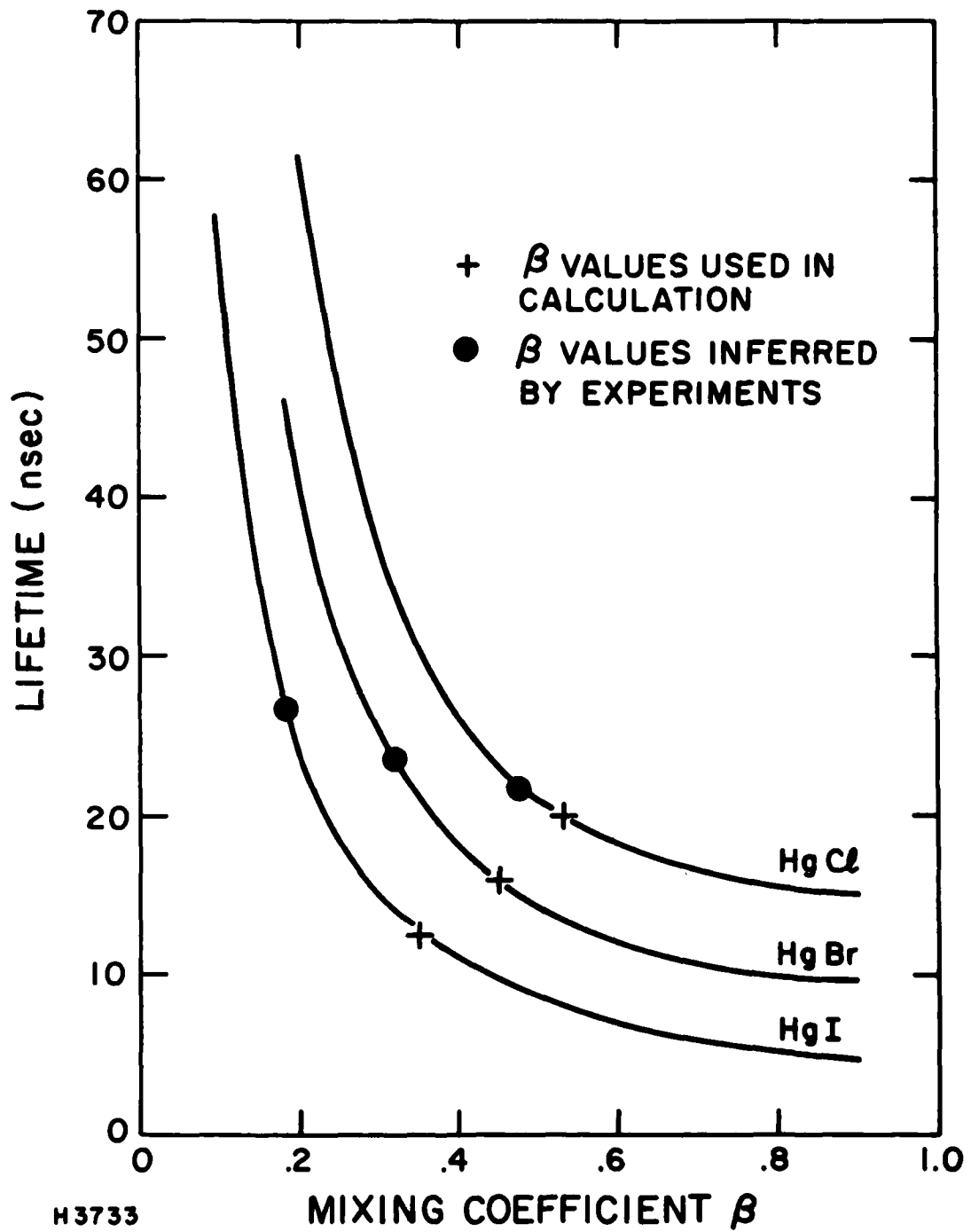


Figure 4. $B \rightarrow X$ Radiative Lifetime of HgX^* as a Function of the Ionic Mixing Coefficient, β

Figure 4 by the cross. From our earlier arguments, we expect these mixing coefficients in Table 2 to be overestimates, so that from Figure 4 the calculated lifetimes are expected to be somewhat too small. This is consistent with the comparison between theory and experiment for HgBr and HgI. The sensitivity of the radiative lifetime to a variation of the mixing coefficient β can be estimated from Figure 4. The β values used in the calculation are observed to be larger than the β values inferred by the experimental measurements consistent with earlier discussion.

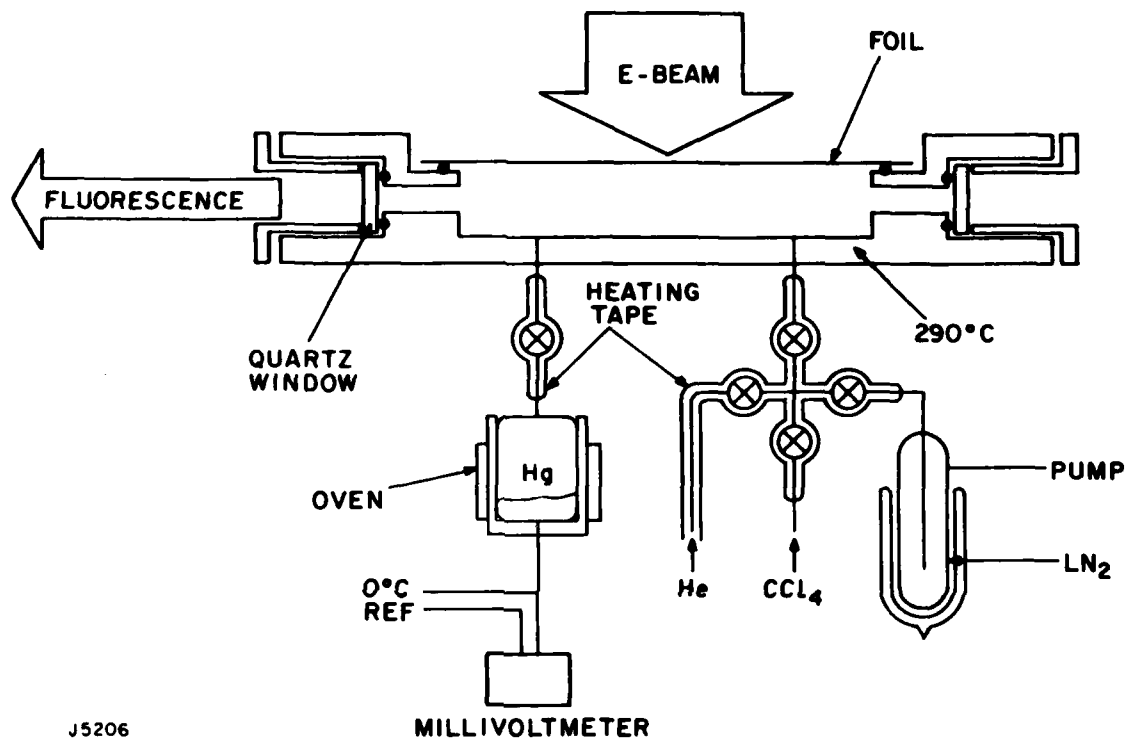
Finally, an estimate of the importance of effects such as HgX* polarization and the broadband emission spectrum were considered and are included in Ref. 27. It should be pointed out that spin-orbit effects have been neglected. While this effect is expected to be small for HgCl, it may become more important for the heavier halides HgBr and in particular HgI.

C. HgX* QUENCHING BY Hg

Several studies have been undertaken to measure the heavy particle quenching rate constant relevant to the mercury halide ($B^2\Sigma_{1/2}^+ \rightarrow X^2\Sigma_{1/2}^+$) laser system. These experiments involved the measurement of either the steady state fluorescence or the time resolved decay of HgX* fluorescence obtained from the photolysis of HgX₂ (28,29,30) or the reaction of photolytically prepared Hg(6^3P_1) with Cl₂. (31) However, because of difficulties inherent in these experiments, there remains considerable uncertainty concerning the rate of relaxation by Hg. A different approach was taken to obtain an independent measurement of the Hg + HgX* rate constant.

In the experiments reported in this letter, the HgCl* (HgBr*) was prepared by reacting Hg⁺ and Cl⁻ (Br⁻). The ionic species were formed by electron beam excitation of a He/Hg/CCl₄ (CF₃Br) mixture. A schematic of apparatus is shown in Figure 5. The reaction cell is made of aluminum, and is maintained at 290°C, along with the quartz windows, by cartridge heaters in the cell body and window mounts. The e-beam (14 A/cm², 250 KeV) enters the cell through a 2 mil kapton foil. The pressure of mercury in the cell was adjusted by controlling the temperature of the mercury reservoir. The He and CCl₄ (CF₃Br) were premixed and preheated in the filling manifold, and expanded into the reaction cell after the Hg was added.

The HgCl (HgBr*) fluorescence was measured using an RCA-C7164R photomultiplier. An example of the fluorescence data is shown in the oscillogram in Figure 6. The fluorescence signal is observed to closely follow the envelope of the current trace (smaller variations in the current trace result from signal mismatch). Data used in analysis were taken at the peak signal value. In order to eliminate x-ray and RF noise, the PMT was contained in a RF shielded housing inside a lead box. Filters were used to eliminate excited Hg line emission. In the case of HgBr*, this filter was broadband and passed the entire HgBr* emission. A



J5206

MILLIVOLTMETER

Figure 5. Schematic of the Experimental Apparatus

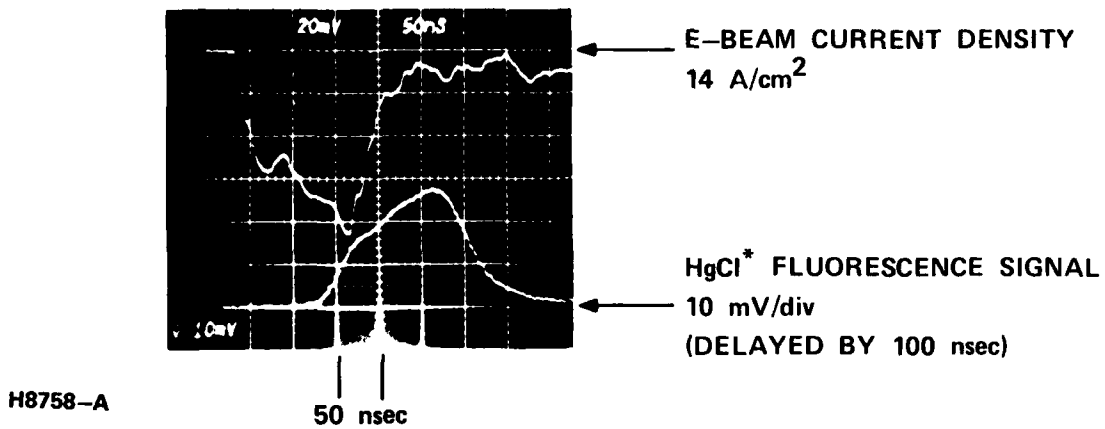
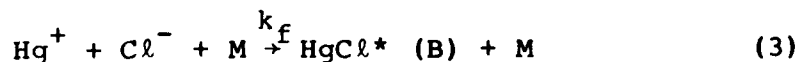
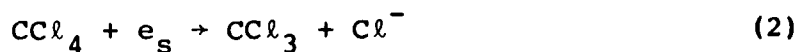


Figure 6. Oscilloscope of a Typical HgCl* Signal and the Associated Trace of E-Beam Current Density

narrow band pass (2.2 nm) filter centered on the HgCl* band maximum was necessary to eliminate the nearby 246 nm Hg* line.

The principal reactions in the production of HgCl* are the following.



The primary electrons, e_p , from the e-beam interact with the Hg to form Hg^+ plus secondary electrons, e_s . These low energy electrons then interact with the CCl_4 to form the Cl^- . The Hg^+ and Cl^- then react in the presence of a stabilizing species M to form the $\text{B}^2\Sigma_{1/2}^+$ state of HgCl.

HgCl* can then either radiate or be deactivated to the ground state by some quenching species Q,



The steady state solution of the corresponding rate equations yield the following expression for the fluorescence intensity:

$$I_{\text{HgCl}^*} = [\text{HgCl}^*] \frac{1}{\tau_r} = \frac{\beta [\text{Hg}]}{1 + k_2 \tau_r [\text{CCl}_4] + k_3 \tau_r [\text{He}] + k_1 \tau_r [\text{Hg}]} \quad (6)$$

where

$$\beta [\text{Hg}] = k_f [\text{Hg}^+] [\text{Cl}^-] = S_{\text{eb}} \quad (7)$$

Rearranging this expression:

$$\frac{[\text{Hg}]}{I_{\text{HgCl}^*}} = \frac{Q \tau_r}{\beta} + \frac{k_1 \tau_r}{\beta} [\text{Hg}] \quad (8)$$

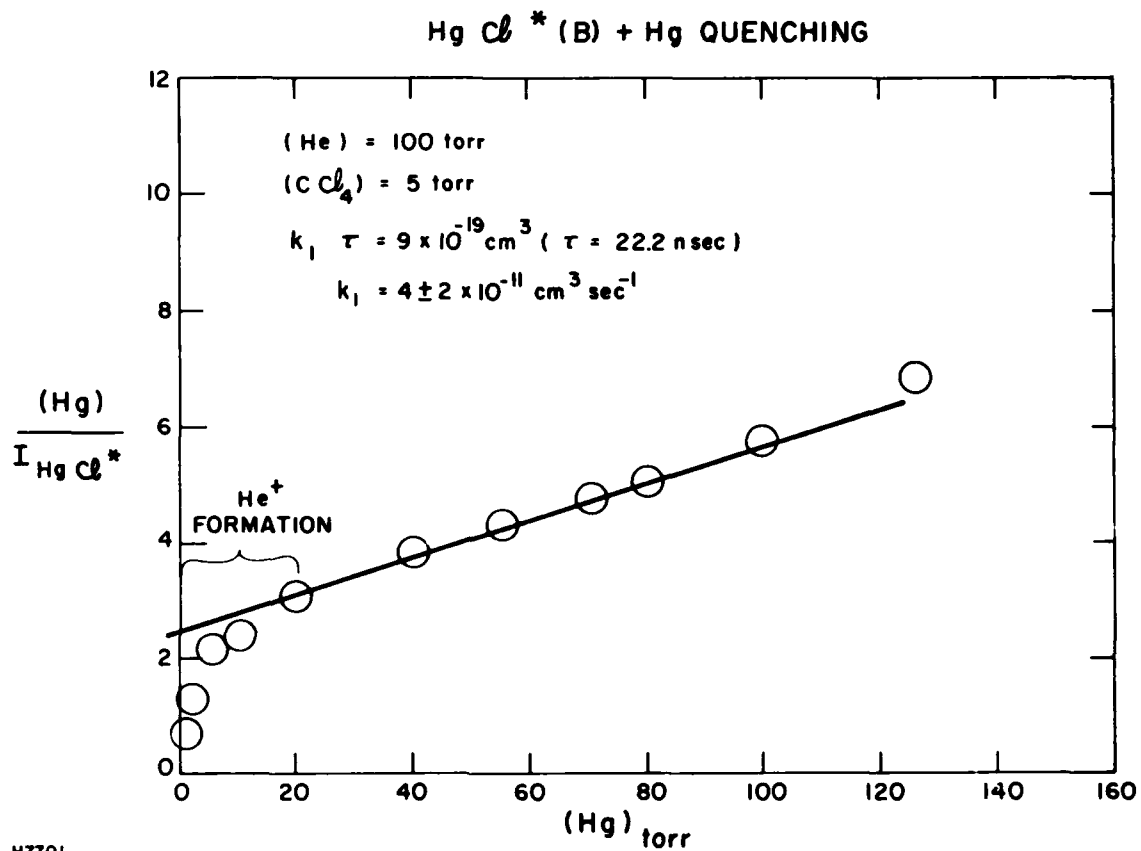
where

where

$$Q \tau_r = 1 + k_2 \tau_r [\text{CCl}_4] + k_3 \tau_r [\text{He}]. \quad (9)$$

The rate constant k_3 for the quenching by Hg can thus be easily obtained from a plot of $[\text{Hg}]/I_{\text{HgCl}^*}$ vs. $[\text{Hg}]$. The experimental results analyzed in this manner are shown in Figure 7. The initial evaluation of the k_1 , Hg relaxation rate constant, from this plot used the CCl_4 rate constant k_2 reported in Ref. 28. The deviation from linearity in the low Hg pressure region observed in Fig. 7 is due to the fact that, at these Hg pressures, a significant fraction of the incident e-beam energy is absorbed by the He. This results in an enhanced Hg^+ formation via a He^+ channel. As a check of the experimental procedure, the quenching rate constant for CCl_4 was obtained from a plot of $1/I_{\text{HgCl}^*}$ vs. $[\text{CCl}_4]$. The experimental results plotted in this fashion are shown in Figure 8. In this analysis the above value of k_1 was used to determine the CCl_4 quenching rate constant k_2 . Similar experiments were performed to determine the rate constants for the quenching of HgBr^* by Hg and CF_3Br .

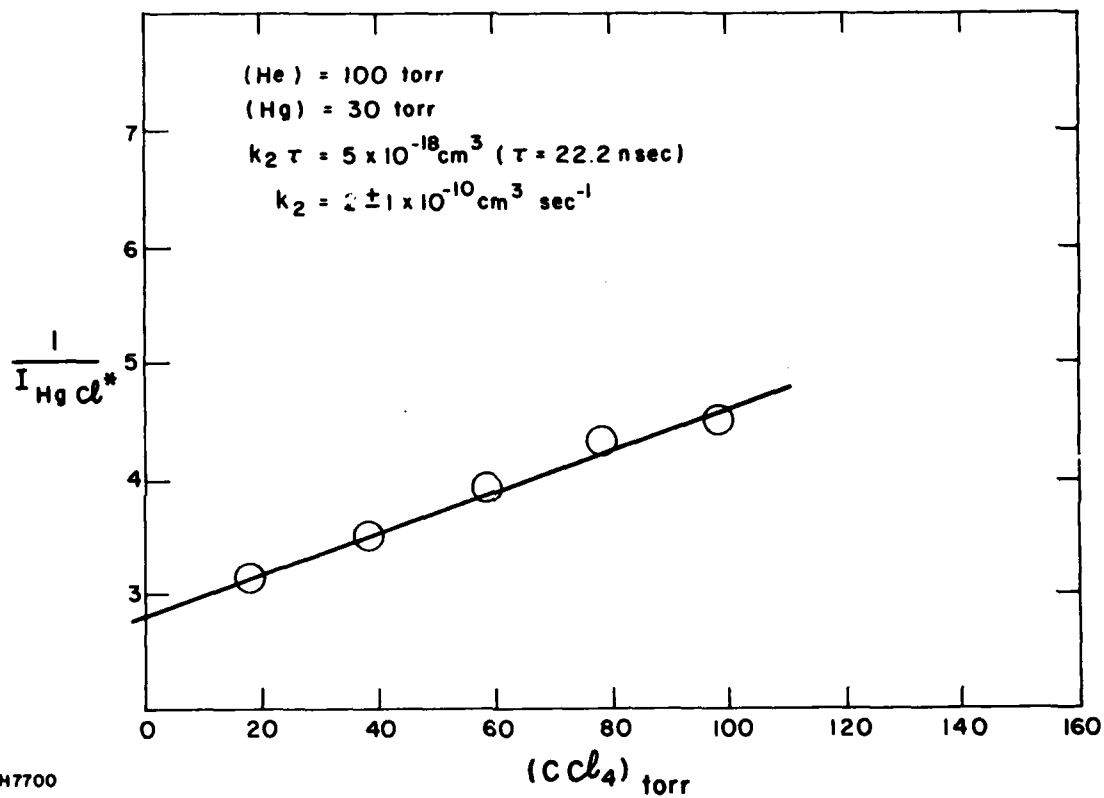
HgCl^* lasing mixtures are commonly .85/.12/.02/.01 Ar, Xe, Hg, CCl_4 with a total density of 3 amagats. Under these conditions the HgCl^* is vibrationally relaxed into the lower vibrational levels of the $B^2\Sigma_{1/2}^+$ state. This being the case, the relative quenching rate constant is that associated with the quenching of these lower vibrational levels. Spectra taken of the HgCl^* emission under typical conditions, 20 Torr Hg, 5 Torr CCl_4 , 200 Torr He showed the structure characteristic of a vibrationally relaxed $\text{HgCl}^*(B)$ state. In addition, experiments were conducted which observed $\text{HgCl}^* v' = 0$ emission under varying He pressure. In Ref. 28 it was shown that photolysis of HgCl_2 in 100 torr of He resulted in an unrelaxed spectrum. However, increasing the He pressure up to 500 torr completely relaxed the spectrum. In the present experiment, looking primarily at emission from $v' = 0$, a substantial increase in fluorescence intensity with increasing He pressure was expected as relaxation occurred. A significant increase was not observed,



H7701

Figure 7. Plot of Experimental Data Showing Best Linear Fit and the Resulting Quenching Rate Constant k_1

Hg Cl* (B) + CCl₄ QUENCHING



H7700

Figure 8. Plot of Experimental Data Showing Best Linear Fit and the Resulting Quenching Rate Constant k_2

as shown in Figure 9, indicating that with the $\text{Hg}^+ + \text{Cl}^-$ formation process, and with the relatively high Hg pressures used in these experiments, vibrational relaxation is complete on the time scale of these experiments.

In light of recent experiments of XeF^* quenching,⁽³²⁾ it is necessary to investigate the possibility of electron quenching of HgX^* . Qualitative experiments to test for the effects of electron quenching in this system were inconclusive. However, an analysis of the kinetics show that under the conditions of the present experiment electron quenching should be insignificant.

The electron quenching process adds the additional term

$$k_{er} \tau_r e_s$$

to $Q \tau_r$ in Eq. (9). In order for this term to be significant, it must have a magnitude comparable to the other quenching terms. An upper limit on the steady state secondary electron density can be approximated by the expression:

$$[e_s] \leq \frac{\beta [\text{Hg}]}{k_a [\text{CCl}_4]} \quad (10)$$

The numerator can be estimated from the e-beam characteristics and the electron stopping power of Hg. Here, k_a is the dissociative attachment rate constant for e_s with CCl_4 . This rate constant was calculated to be $\sim 1 \times 10^{-8} \text{ cm}^3 \text{ sec}^{-1}$ from the energy dependence of the cross section^(33,34) and a Boltzmann code calculation of the electron energy distribution. Using Eq. (10), an upper limit on the secondary electron density is $[e_s] \sim 2 \times 10^{12} \text{ cm}^{-3}$. In this limit, k_{er} would have to be greater than $1 \times 10^{-4} \text{ cm}^3 \text{ sec}^{-1}$ to influence the quenching rate constants measured in this experiment. Since this is an unrealistically large rate constant, corrections for electron quenching effects in this experiment are not considered necessary.

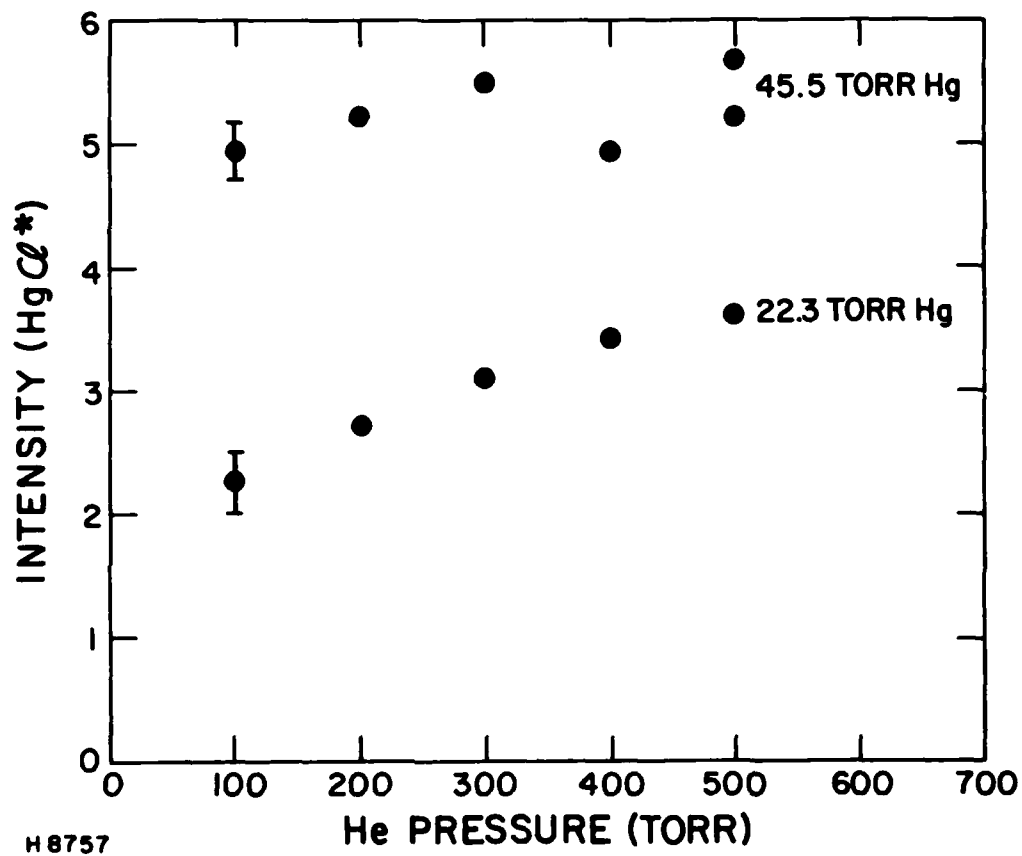


Figure 9. HgCl* Fluorescence vs Helium Pressure at Mercury Densities Corresponding to 45.5 and 22.3 Torr

The rate constants measured in these experiments are summarized in Table 3. The radiative lifetime of 22.2 nsec⁽¹⁸⁾ was used to evaluate the rate constant involving HgCl* and 23.7 nsec^(19,20) for those involving HgBr*. Also included in Table 3 are the corresponding values obtained elsewhere. Note that there is good agreement on those rate constants not involving Hg. There is however an order of magnitude disagreement with Eden and Waynant on the quenching of HgBr* by Hg. At this time there is no explanation for this difference. However, as was pointed out in Ref. 29, a rate constant $\sim 10^{-11} \text{ cm}^3 \text{ sec}^{-1}$ is expected considering the corresponding quenching rates in the ArF*⁽³⁵⁾ and XeF*⁽³⁶⁾ excimer systems. In addition, the Eden and Waynant rate constant for HgCl*(B) quenching by N₂ was an order of magnitude larger than other measurements.^(28,30) This suggests the possibility that impurity quenching may be dominating their measurement in some instances.

TABLE 3. RATE CONSTANTS MEASURED FOR VARIOUS QUENCHING REACTIONS. RESULTS FROM REFERENCED EXPERIMENTS ARE SHOWN FOR COMPARISON.

<u>Quenching Reaction</u>	<u>Rate Constant (present experiment) (cm³ sec⁻¹)</u>	<u>Rate Constant (ref. experiment) (cm³ sec⁻¹)</u>
HgCl* + Hg	4.6 (± 1) x 10 ⁻¹¹	—
HgCl* + CCl ₄	2.3 (± .3) x 10 ⁻¹⁰	1.6 x 10 ⁻¹⁰ (1)
HgBr* + Hg	1.4 (± 1) x 10 ⁻¹¹	1.3 x 10 ⁻¹⁰ (2)
HgBr* + CF ₃ Br	1.2 (± .4) x 10 ⁻¹⁰	8.9 x 10 ⁻¹¹ (14)

REFERENCES

1. Smith, D., Dean, A.G., and Plumb, I.C., J. Phys. B5, 2134 (1972).
2. Biondi, M.A., Mercury Halide Kinetics Review, Univ. So. Calif. March 1, 1979.
3. Bohme, D.K., Adams, N.G., Moselman, M., Dunkin, D., and Ferguson, E.E., J. Chem. Phys. 52, 5094 (1970).
4. Christophorou, L.G. and Stockdale, J.A.D., J. Chem. Phys. 48, 1956 (1968). Spence, D. and Schulz, G.J., J. Chem. Phys. 58, 1800 (1973).
5. Flannery, M.R., Chem. Phys. Lett. 56, 143 (1978).
6. Rokni, M., Jacob, J.H., Mangano, J.A., and Brochu, R., Appl. Phys. Lett. 31, 26 (1977).
7. Mangano, J.A., Jacob, J.H., Rokni, M. and Hawryluk, A., Appl. Phys. Lett. 31, 26 (1977).
8. Krause, H.F., Johnson, S.G., Datz, S. and Schmidt-Bleek, F.K., Chem. Phys. Lett. 31, 577 (1975).
9. Zamir, E., Huestis, D.L., Lorents, D.C. and Nakano, N.H., in Electrical Transition Lasers II edited by L.E. Wilson, S.N. Suchard, and J.I. Steinfeld, MIT Press, Cambridge, Massachusetts 1977, p 69.
10. Gleason, R.E., Bonifield, T.D., Keto, J.W. and Walters, G.K., J. Chem. Phys. 66, 1589 (1977).
11. Gedanken, A. Jortner, J., Rax, B. and Szoki, A., J. Chem. Phys. 57, 3456 (1972).
12. Hay, P. and Dunning, T., Jr., J. Chem. Phys. 66, 1306 (1977).
13. Mulliken, R.S., J. Chem. Phys. 7, (1939) 20.
14. Zare, R.N. and Herschbach, D.R., J. Mol. Spectry, 15 (1965) 462.
15. Ewing, J.J. and Brau, C.A., Phys. Rev. A12, 129 (1975).
16. Herzber, G. Spectra of Diatomic Molecules, 2nd ed. (Van Nostrand, Princeton, 1950).

17. Coulson, C.A., Valence, 2nd ed. (Oxford Univ. Press, London, 1961) pp. 139-141.
18. Eden, J.G., Appl. Phys. Lett. 33, 495 (1978).
19. Djeu, N., Mazza, C., Chem. Phys. Lett. 46, 172 (1977).
20. Waynant, R.W., Eden, J.G., Appl. Phys. Lett. 33, 708 (1978).
21. Clementi, E. and Roetti, C., At. Nucl. Data Tables 14 (1974) 177.
22. Burke, V.M. and Grant, I.P., Proc, Phys. Soc. (London) 90 (1967) 297.
23. Herman, F. and Skillman, S., Atomic Structure Calculations (prentice-Hall, Englewood Cliffs, 1963).
24. Lu, C.C., Carlson, T.A., Malik, F.B., Tucker, T.C. and Nestor, C.W., Jr., At. Data 3 (1971) 1.
25. Sharma, R.R., Phys. Rev. A13, (1976) 517.
26. Wieland, K., Helv. Phys. Acta. 14 (1941) 420.
27. Duzy, C., Hyman, H.A., Chem. Phys. Lett. 52, 345 (1977).
28. Mandl, A. and Parks, J.H., Appl. Phys. Lett. 33, 498 (1978).
29. Eden, J.G. and Waynant, R.W., Appl. Phys. Lett. 34, 324 (1979).
30. Halvajian, H. and Wittig, C., Opt. Comm. in press.
31. Tang, K.Y., Hunter, R.O. and Oldenettel, J., J. Chem. Phys. 70, 1492 (1979).
32. Trainor, D.W., Jacob, J.H., Rokni, M., J. Chem. Phys. 72, 3646 (1980).
33. Fox, R.E. and Curran, R.K., J. Chem. Phys. 34, 1595 (1961).
34. Christophoron, L.G. and Stockdale, J.A.D., J. Chem. Phys. 48, 1956 (1968).
35. Rokni, M., Jacob, J.H. and Mangano, J.A., Phys. Rev. A 16, 2216 (1977).
36. Brashears, Jr. H.C., Setser, D.W. and Desmartean, D., Chem. Phys. Lett. 48, 84 (1977).

DISTRIBUTION LIST

Office of Naval Research, Department of the Navy, Arlington, VA 22217 - Attn: Physics Program (1 copy)
 Naval Research Laboratory, Department of the Navy, Washington, D.C. 20375 - Attn: Technical Library (1 copy)
 Office of the Director of Defense, Research and Engineering, Information Office Library Branch, The Pentagon
 Washington, D.C. 20301 - (1 copy)

U.S. Army Research Office, Box CM, Duke Station, Durham, N.C. 27706 - (1 copy)
 Defense Documentation Center, Cameron Station, Alexandria, VA 22314 - (1 copy)
 Defender Information Analysis Center, Battelle Memorial Institute, 505 King Avenue, Columbus, OH 43201 - (1 copy)
 Commanding Officer, Office of Naval Research Branch Office, 536 South Clark Street, Chicago, IL 60615 - (1 copy)
 New York Area Office, Office of Naval Research, 715 Broadway (5th Floor), New York, NY 10003 -
 Attn: Dr. Irving Rowe (1 copy)

Air Force Office of Scientific Research, Department of the Air Force, Washington, D.C. 22209 - (1 copy)
 Office of Naval Research Branch Office, 1030 East Green Street, Pasadena, CA 91106 - Attn: Dr. Robert Behringer
 (1 copy)

Defense Advanced Research Projects Agency, 1400 Wilson Blvd., Arlington, VA 22209 - Attn: Strategic Technology
 Office (1 copy)

Office Director of Defense, Research and Engineering, The Pentagon, Washington, D.C. 20301 - Attn: Asst. Dir.
 (Space and Adv. Systems) (1 copy)

Office of the Assistant Secretary of Def., System Analysis (Strategic Programs), Washington, D.C. 20301 -
 Attn: Mr. Gerald R. McNichols

U.S. Arms Control and Disarmament Agency, Dept. of the State Bldg., Rm. 4931, Washington, D.C. 20451 Attn: Dr. Charles Henkin - (1 copy)
 Energy Research Development Agency, Division of Military Applications, Washington, D.C. 20545 - (1 copy)
 National Aeronautics and Space Admin., Lewis Research Center, Cleveland, Oh 44135 - Attn: Dr. John W. Dunning, Jr.
 Aerospace Research Engineer
 (1 copy)

National Aeronautics & Space Admin., Code RR, FOB 10B, 600 Independence Ave., SW, Washington, D.C. 20546 - (1 copy)
 National Aeronautics and Space Admin., Ames Research Center, Moffit Field, CA 94035 - Attn: Dr. Kenneth W. Billman
 (1 copy)

Department of the Army, Office of the Chief of RD&A, Washington, D.C. 20310 - Attn: DARD-DD (1 copy)
 Department of the Army, Office of the Chief of RD&A, Washington, D.C. 20310 - Attn: DAMA-WSM-T (1 copy)
 Department of the Army, Office of the Deputy Chief of Staff for Operations and Plans, Washington, D.C. 20310
 Attn: DAMO-RQD (1 copy)

U.S. Army Missile Command, Research and Development Division, Redstone Arsenal, AL 35809 - Attn: Army High
 Energy Laser Programs (1 copy)

Commanding Officer, U.S. Army Mobility Equipment R&D Center, Ft. Belvoir, VA 22060 - Attn: SMEFB-MW (1 copy)
 Commander, U.S. Army Armanent Command, Rock Island, IL 61201 - Attn: AMSAR-RDT (1 copy)
 Director, Ballistic Missile Defense Adv. Technology Center, P.O. Box 1500, Huntsville, AL 35807 -
 Attn: ATC-O (1 copy)
 Director, Ballistic Missile Defense Adv. Technology Center, P.O. Box 1500, Huntsville, AL 35807 -
 Attn: ACT-T

Commanding General, U.S. Army Munitions Command, Dover, NH 17801 - Attn: Mr. Gilbert F. Chesnov (AMSMU-R) (1 copy)
 Director, U.S. Army Ballistics Res. Lab., Aberdeen Proving Ground, MD 21005 - Attn: Dr. Robert Eichenberger (1 copy)
 Commandant U.S. Army, Air Defense School, Ft. Bliss, TX 79916 - Attn: Air Defense Agency (1 copy)
 Commandant, U.S. Army, Air Defense School, Ft. Bliss, TX 79916 - Attn: ATSA-CTD-MS (1 copy)
 Commanding General, U.S. Army Combat Dev. Command, Ft. Belvoir, VA 22060 - Attn: Director of Material,
 Missile Div. (1 copy)

Commander, U.S. Army Training and Doctrine Command, Ft. Monroe, VA 23651 - Attn: ATCD-CF (1 copy)
 Commander, U.S. Army Electronics Command, Ft. Monmouth, NJ 07703, Attn: AMSEL-CT-L, Dr. R.G. Buser (1 copy)
 Commander, U.S. Army Combined Arms Combat Dev. Act., Ft. Leavenworth, KS 66027 - (1 copy)

National Security Agency, Ft., Geo. G. Meade, MD 20755 - Attn: R.C. FOSS A763 (1 copy)
 Deputy Commandant - For Combat and Training Developments, U.S. Army Ordnance Center and School,
 Aberdeen Proving Ground, MD 21005 - Attn: ATSL-CTD-MS-R (1 copy)

Department of the Navy, Office of the Chief of Naval Operations, The Pentagon 50739, Washington, D.C. 20350 -
 Attn: (OP 982F3)

Boston Branch Office, Bldg. 114, Section D, 666 Summer Street, Boston, MA 02210 (1 copy)
 Department of the Navy, Deputy Chief of Navy Material (Dev.), Washington, D.C. 20360 -
 Attn: Mr. R. Gaylord (MAT 032B) (1 copy)

Naval Missile Center, Point Mugu, CA 91042 - Attn: Gary Gibbs (Code 5352) (1 copy)
 Naval Research Laboratory, Washington, D.C. 20375 - Attn: Electro Optical Technology, Program Office,
 Code 1409 (1 copy)

Naval Research Laboratory, Washington, D.C. 20375 - Attn: Dr. P. Livingston - Code 5560 (1 copy)
 Naval Research Laboratory, Washington, D.C. 20375 - Attn: Dr. A.I. Schindler - Code 6000 (1 copy)
 Naval Research Laboratory, Washington, D.C. 20375 - Attn: Dr. John L. Walsh - Code 5503 (1 copy)
 High Energy Laser Project Office, Department of the Navy, Naval Sea System Command, Washington, D.C. 20360 -
 Attn: Capt. A. Skolnick, USN (PM 22) (1 copy)

Superintendent, Naval Postgraduate School, Monterey, CA 93940 - Attn: Library (Code 2124) (1 copy)
 Navy Radiation Technology, Air Force Weapons Lab (NLO), Kirtland AFB, NM 87117 (1 copy)
 Naval Surface Weapons Center, White Oak, Silver Spring, MD 20910 - Attn: Dr. Leon H. Schindel
 (Code 310) (1 copy)

DISTRIBUTION LIST (Continued)

Naval Surface Weapons Center, White Oak, Silver Spring, MD 20910 - Attn: Dr. E. Leroy Harris (Code 313) (1 copy)
 Naval Surface Weapons Center, White Oak, Silver Spring, MD 20910 - Attn: Mr. K. Enkenhaus (Code 034) (1 copy)
 Naval Surface Weapons Center, White Oak, Silver Spring, MD 20910 - Attn: Mr. J. Wise (Code 047) (1 copy)
 Naval Surface Weapons Center, White Oak, Silver Spring, MD 20910 - Attn: Technical Library (1 copy)
 U.S. Naval Weapons Center, China Lake, CA 93555 - Attn: Technical Library (1 copy)
 HQ AFSC/XRLW, Andrews AFB, Washington, D.C. 20331 - Attn: Maj. J.M. Walton (1 copy)
 HQ AFSC (DLCAW), Andrews AFB, Washington, D.C. 20331 - Attn: Maj. H. Axelrod (1 copy)
 Air Force Weapons Laboratory, Kirtland AFB, NM 87117 - Attn: LR (1 copy)
 Air Force Weapons Laboratory, Kirtland AFB, NM 87117 - Attn: AL (1 copy)
 HQ Aeronautical Systems Div., Wright Patterson AFB, OH 45433 - Attn: XRF - Mr. Clifford Fawcett (1 copy)
 Rome Air Development Command, Griffiss AFB, Rome, NY 13440 - Attn: Mr. R. Urtz (OCSE) (1 copy)
 HQ Electronics Systems Div. (ESL), L.G. Hanscom Field, Bedford, MA 01730 - Attn: Mr. Alfred E. Anderson (XRT) (1 copy)
 HQ Electronics Systems Div. (ESL), L.G. Hanscom Field, Bedford, MA 01730 - Attn: Technical Library (1 copy)
 Air Force Rocket Propulsion Lab., Edwards AFB, CA 93523 - Attn: B.R. Bornhorst, (LKCG) (1 copy)
 Air Force Aero Propulsion Lab., Wright Patterson AFB, OH 45433 - Attn: Col. Walter MOE (CC) (1 copy)
 Dept. of the Air Force, Foreign Technology Division, Wright Patterson AFB, OH 45433 - Attn: PDTN (1 copy)
 Commandant of the Marine Corps., Scientific Advisor (Code RD-1), Washington, D.C. 20380 (1 copy)
 Aerospace Research Labs., (AP), Wright Patterson AFB, OH 45433 - Attn: Lt. Col. Max Duggins (1 copy)
 Defense Intelligence Agency, Washington, D.C. 20301 - Attn: Mr. Seymour Berler (DTIB) (1 copy)
 Central Intelligence Agency, Washington, D.C. 20505 - Attn: Mr. Julian C. Nall (1 copy)
 Aircresearch Manuf. Co., 9851-9951 Sepulveda Blvd., Los Angeles, CA 90009 - Attn: Mr. A. Colin Stancliffe (1 copy)
 Atlantic Research Corp., Shirley Highway at Edsall Road, Alexandria, VA 22314 - Attn: Mr. Robert Naismith (1 copy)
 Battelle Columbus Laboratories, 505 King Avenue, Columbus, OH 43201 - Attn: Mr. Fed Tietzel (STPIAC) (1 copy)
 Bell Aerospace Co., Buffalo, NY 14240 - Attn: Dr. Wayne C. Solomon (1 copy)
 Boeing Company, P.O. Box 3999, Seattle, WA 98124 - Attn: Mr. M.I. Gamble (2-460,MS 8C-88) (1 copy)
 Electro-Optical Systems, 300 N. Halstead, Pasadena, CA 91107 - Attn: Dr. Andrew Jensen (1 copy)
 General Electric Co., Space Division, P.O. Box 8555, Philadelphia, PA 19101 - Attn: Dr. R.R. Sigismonti (1 copy)
 General Electric Co., 100 Plastics Avenue, Pittsfield, MA 01201 - Attn: Mr. D.G. Harrington (Ra. 1044) (1 copy)
 Hercules, Inc., Industrial Dept., Wilmington, DE 19899 - Attn: Dr. R.S. Voris (1 copy)
 Hercules, Inc., P.O. Box 210, Cumberland, MD 21502 - Attn: Dr. Ralph R. Preckel (1 copy)
 Hughes Research Labs., 3011 Malibu Canyon Road, Malibu, CA 90265 - Attn: Dr. D. Forster (1 copy)
 Hughes Aircraft Co., Aerospace Group-Systems Division, Canoga Park, CA 91304 - Attn: Dr. Jack A. Alcalay (1 copy)
 Hughes Aircraft Co., Centinela and Teale Streets, Building 6, MS E-125, Culver City, CA 90230 -
 Attn: Dr. William Yates (1 copy)
 Institute for Defense Analyses, 400 Army-Navy Drive, Arlington, VA 22202 - Attn: Dr. Alvin Schnitzler (1 copy)
 Lawrence Livermore Laboratory, P.O. Box 808, Livermore, CA 94550 - Attn: Dr. R.E. Kidder (1 copy)
 Lawrence Livermore Laboratory, P.O. Box 808, Livermore, CA 94550 - Attn: Dr. E. Teller (1 copy)
 Lawrence Livermore Laboratory, P.O. Box 808, Livermore, CA 94550 - Attn: Dr. Joe Fleck (1 copy)
 Los Alamos Scientific Laboratory, P.O. Box 1663, Los Alamos, NM 87544 - Attn: Dr. Keith Boyer (1 copy)
 Lockheed Palo Alto Research Lab., 3251 Hanover Street, Palo Alto, CA 94303 - Attn: L.R. Lunsford,
 Orgn. 52-24, Bldg. 201 (1 copy)
 Mathematical Sciences Northwest, Inc., P.O. Box 1887, Bellevue, WA 98009 - Attn: Dr. Abraham Hertzberg (1 copy)
 Massachusetts Institute of Technology, Lincoln Laboratory, P.O. Box 73, Lexington, MA 02173 -
 Attn: Dr. S. Edelberg (1 copy)
 Massachusetts Institute of Technology, Lincoln Laboratory, P.O. Box 73, Lexington, MA 02173 -
 Attn: Dr. L.C. Marquet (1 copy)
 McDonnell Douglas Astronautics Co., 5301 Bolsa Avenue, Huntington Beach, CA 92647 -
 Attn: Mr. P.L. Klevatt, Dept. A3-830-BBFO, M/Sg (1 copy)
 McDonnell Douglas Research Labs., Dept. 220, Box 516, St. Louis, MO 63166 - Attn: Dr. D.P. Ames (1 copy)
 Dr. Anthony N. Pirri, 30 Commerce Way, Woburn, MA 01801 (1 copy)
 Rand Corp., 1700 Main Street, Santa Monica, CA 90406 - Attn: Dr. C.R. Culp/Mr. G.A. Carter (1 copy)
 Raytheon Co., 28 Seyon Street, Waltham, MA 02154 - Attn: Dr. P.A. Horrigan (Res. Div.) (1 copy)
 Raytheon Co., Boston Post Road, Sudbury, MA 01776 - Attn: Dr. C. Sonnenschien (Equip. Div.) (1 copy)
 Raytheon Co., Bedford Labs, Missile Systems Div., Bedford, MA 01730 - Attn: Dr. H.A. Mehlhorn (1 copy)
 Riverside Research Institute, 80 West End Street, New York, NY 10023 - Attn: Dr. L.H. O'Neill (1 copy)
 Riverside Reserach Institute, 80 West End Street, New York, NY 10023 - Attn: Dr. John Bose (1 copy)

DISTRIBUTION LIST (Continued)

Riverside Reserach Institute, 80 West End Street, New York, NY 10023 - Attn: (HPEGL Library) (1 copy)
Rockwell International Corporation, Rocketdyne Division, Albuquerque District Office, 3636 Menaul Blvd.,
Ne, Suite 211, Albuquerque, NM 87110 - Attn: C.K. Kraus, MGR. (1 copy)
Sandia Corp., P.O. Box 5800, Albuquerque, NM 87115 - Attn: Dr. Al Narath (1 copy)
Stanford Reserach Institute, Menlo Park, CA 94025 - Attn: Dr. F.T. Smith (1 copy)
Science Applications, Inc., 1911 N. Ft. Meyer Drive Arlington, VA 22209 - Attn: L. Peckham (1 copy)
Science Applications, Inc., P.O. Box 328, Ann Arbor, MI 48103 - Attn: R.E. Meredith (1 copy)
Science Applications, Inc., 6 Preston Court, Bedford, MA 01703 - Attn: R. Greenberg (1 copy)
Science Applications, Inc., P.O. Box 2351, La Jolla, CA 92037 - Attn: Dr. John Asmus (1 copy)
Systems Science and Software, P.O. Box 1620, La Jolla, CA 92037 - Attn: Alan F. Klein (1 copy)
Systems Consultants, Inc., 1050 31st Street, NW, Washington, D.C. 20007 - Attn: Dr. R.B. Keller (1 copy)
Thiokol Chemical Corp., Wasatch Division, P.O. Box 524, Brigham City, UT 84302 - Attn: Mr. J.E. Hansen (1 copy)
TRW Systems Group, One Space Park, Bldg. R-1, Rm. 1050, Redondo Beach, CA 90278 - Attn: Mr. Norman Campbell (1 copy)
United Technologies Research Center, 400 Main Street, East Hartford, CT 06108 - Attn: Mr. G.H. McLafferty (1 copy)
United Technologies Reserach Center, Pratt and Whitney Aircraft Div., Florida R&D Center, West Palm Beach, FL 33402,
Attn: Dr. R.A. Schmidke (1 copy)
United Technologies Research Center, Pratt and Whitney Aircraft Div., Florida R&D Center, West Palm Beach, FL 33402,
Attn: Mr. Ed Pinsley
Varian Associates, EIMAC Division, 301 Industrial Way, San Carlos, CA 94070 - Attn: Mr. Jack Quinn (1 copy)
Vought Systems Division, LTV Aerospace Corp., P.O. Box 5907, Dallas, TX 75222 - Attn: Mr. F.G. Simpson, MS254142
(1 copy)
Westinghouse Electric Corp., Defense and Space Center, Balt-Wash. International Airport, Box 746,
Baltimore, MD 21203 - Attn: Mr. W.F. List (1 copy)
Westinghouse Research Labs., Beulah Road, Churchill Boro, Pittsburgh, PA 15235 - Attn: Dr. E.P. Riedel (1 copy)
United Technologies Research, East Hartford, CT 06108 - Attn: A.J. DeMaria (1 copy)
Aireborne Instruments Laboratory, Walt Whitorian Road, Melville, NY 11746 - Attn: F. Pace (1 copy)
General Electric R&D Center, Schenectady, NY 12305 - Attn: Dr. Donald White (1 copy)
Cleveland State University, Cleveland, OH 44115 - Attn: Dean Jack Soules (1 copy)
Exxon Research and Engineering Co., P.O. Box 8 Linden, NJ 07036 - Attn: D. Grafstein (1 copy)
University of Maryland, Department of Physics and Astronomy, College Park, MD 20742 - Attn: D. Currie (1 copy)
Sylvania Electric Products Inc., 100 Fergeson Drive, Montian View, CA 94040 - Attn: L.M. Osterink (1 copy)
North American Rockwell Corp., Autonetics Division, 3370 Miraloma Avenue, Anaheim, CA 92803 -
Attn: R. Gudmundsen (1 copy)
Massachusetts Institute of Technology, 77 Massachusetts Avenue, Cambridge, MA 02138 - Attn: Prof. A. Javan (1 copy)
Lockheed Missile & Space Co., Palo Alto Research Laboratories, Palo Alto, CA 94304 - Attn: Dr. R.C. Ohlman (1 copy)
Polytechnic Institute of New York, Rt. 110, Farmingtondale, NY 11735 - Attn: Dr. William T. Walter (1 copy)